Published in final edited form as:
Biomaterials. 2010 December ; 31(34): 8902–8910. doi:10.1016/j.biomaterials.2010.07.109.

Osteoinductive silk-silica composite biomaterials for bone regeneration

Aneta J. Mieszawska[1], **Nikolaos Fourligas**[1], **Irene Georgakoudi**[1], **Nadia Ouhib**[2], **David J. Belton**[3], **Carole C. Perry**[3], and **David L. Kaplan**[1,*]

[1]Department of Biomedical Engineering, 4 Colby Street, Tufts University, Medford, MA 02155, United States

[2]Department of Biomedical Engineering, Boston University, 44 Cummington Street, Boston, MA 02215

[3]School of Science and Technology,, Nottingham Trent University, Clifton Lane, Nottingham, NG11 8NS. UK

Abstract

Osteoinductive and biodegradable composite biomaterials for bone regeneration were prepared by combining silk fibroin with silica particles. The influence of these composite systems on osteogenesis was evaluated with human mesenchymal stem cells (hMSCs) subjected to osteogenic differentiation. hMSCs adhered, proliferated, and differentiated towards osteogenic lineages on silk/silica films. The addition of the silica to the silk films influenced gene expression leading to upregulation of bone sialoprotein (BSP) and collagen type 1 (Col 1) osteogenic markers. Evidence for early bone formation in the form of collagen fibers and apatite nodules was obtained on the silk/silica films. Collagen fibers were closely associated with apatite deposits and overall collagen content was higher for the silica containing samples. Also, smaller sized silica particles (24 nm – 2 μm) with large surface area facilitated silica biodegradation *in vitro* through particle dissolution, leading to ~5 fold decrease in silica content over 10 weeks. These results indicate suitability of silk/silica composite system towards bone regeneration, where degradation/remodeling rates of the organic and inorganic components can be controlled.

Introduction

The focus of biomaterial designs for tissue engineering applications has recently been directed towards bioactive components that facilitate biomaterial integration and native tissue regeneration at the implant site [1]. Bone remodeling, both *in vitro* and *in vivo*, depends strongly on the development of such materials that would bear the load of hard tissue and stimulate osteogenic cells towards bone regeneration concurrently [2,3]. Most commercially available bone substituents are derived from calcium phosphate ceramics, titanium or bioactive glasses [4-6]. Despite their numerous advantages they often fail to fulfill all the desired properties that are sought in biomaterials for bone regeneration, with either a lack of biological activity, low durability, a mechanical mismatch with surrounding tissue or a lack of biodegradation.

*Corresponding author. David.Kaplan@tufts.edu.

Silk fibroin isolated from *Bombyx mori* silkworm cocoons is a promising biomaterial that has been used for both *in vitro* and *in vivo* tissue engineering applications [7,8]. The mechanical strength, biocompatibility, and slow degradation rate that facilitates material substitution with newly formed tissue, suggest that silk is suitable for use as a matrix material in bone regeneration studies. The impressive mechanical properties of silk originate from the formation of beta-sheet secondary structures. These crystals add to protein stability in organic solvents or aqueous environments, with degradation dependent on proteolytic activity. The β-sheet conformation can be induced through chemical or physical treatments that, depending on the method, lead to different degrees of β-sheet crystallization giving fine control over silk degradation rates [9-13]. Additionally, silks offer multiple methods for processing into biomaterials and can be formed into films, hydrogels, fibers, sponges or scaffolds from aqueous processes [14-18]. Thus silk is suitable for use as a matrix material in bone regeneration [19-22]. Silk alone is not osteoinductive, thus improvements in bone regeneration can be anticipated by the addition of osteoinductive features.

Silica-based glasses have been extensively studied as skeletal repair materials due to their high bioactivity and ability to bind strongly to bone [23-25]. Nevertheless, the use of bioactive glasses is limited due to the lack of biodegradability that hampers the regeneration process by blocking new tissue ingrowth and regeneration. Recent advances in nanotechnology have led to the fabrication of nanostructural silica-based materials that have been studied for biological applications [26]. High surface area of nano-sized silica and availability of silanol groups (Si-OH) for functionalization have led to silica particle uses in cell targeting and drug delivery, as well as in biosensing and bioimaging [26-28]. Bioactive glass nanostructures showed promise for bone regeneration studies [25,29-31].

In the present study the goal was to combine the useful biomaterial properties of both silk and silica for composite organic/inorganic biomaterials for bone tissue engineering applications. We focused on nanometer sized silica particles embedded in silk matrix material for the study to optimize potential degradation and remodeling. These new silk/silica systems provide a bioactive, mechanically strong, and biodegradable bone substitute biomaterial.

2. Methods and materials

All chemicals were purchased from Sigma-Aldrich (MO, USA) or Fluka (WI, USA) and used without further purification. Cell medium ingredients were purchased from Invitrogen (CA, USA) and Sigma-Aldrich (MO, USA). Cocoons from *Bombyx mori* silkworm were obtained from Tajima Shoji Co (Yokohama, Japan). Surface morphology down to the nanometer levels was evaluated using a Carl Zeiss (Carl Zeiss SMT, Germany) Ultra 55 Field Emission Scanning Electron Microscope (FESEM) operating at an accelerating voltage of 10 kV and using an in-lens ion annular secondary electron detector. The bottom of the tissue culture plate (TCP) well with cast film was cut and coated with a carbon layer (Baltec Carbon Coater, model MED-020, Liechtenstein) to ensure sample conductivity necessary for imaging. The SEM was operated under high vacuum at 10 and 20 keV with typical currents of 10 keV. Elemental composition of the silk film surface was evaluated using an Energy Dispersive X-ray Spectrometer (EDAX) connected to the SEM instrument.

2.1. Preparation of silk proteins

The protein powders were obtained using previously published protocols [19]. Briefly, cocoons from the *B. mori* silkworm were cut and boiled for 1 h in an aqueous solution of 0.02 M Na_2CO_3, rinsed once with boiling water then three times with room temperature distilled water. The purified silk fibroin was then solubilized by dissolving in 9 M LiBr solution at 60°C for 45 min to give a 20 wt% solution. This solution was filtered through a 5 μm syringe filter, then dialyzed (membrane MWCO 3,500 g mol^{-1}; Pierce, Woburn, MA) against distilled water for

3 days changing the water 3 times a day. The silk solutions had a final concentration of 9-11 wt% and were freeze dried to obtain the protein powder.

2.2. Synthesis of silica particles

The sizes of silica particles were studied, 24 nm, 500 nm and 2 um. The silica particles (24 nm and 500 nm) were synthesized using a variant of the Stöber method [32], wherein solutions of tetraethoxysilane (0.1M) in ethanol and ammonia (0.05-10M final concentration of ammonia in distilled and deionized water, to vary the particle sizes produced) were heated to 50°C then mixed with stirring for 80 minutes (temperature maintained at 50°C) and the particle sizes determined by photon correlation spectroscopy after this time. The condensed silica spheres were then isolated by removal of excess ammonia at ambient pressure and temperature and reduction of ethanol content to approximately half volume. The suspensions were then re-diluted to their original volume with distilled-deionized water followed by freeze drying. The 2 μm ± 0.2 μm silica particles were purchased from Fluka (WI, USA).

2.3. Preparation of silk and silk/silica films

Hexafluoro-2-propanol (HFIP) based silk fibroin solutions were prepared at a concentration of 2.5% wt/vol and stirred overnight to ensure complete protein dissolution. The silk solutions were filtered using a 0.22 μm syringe filter in a tissue culture hood. The three different silica particle sizes were suspended in water at a concentration of 2.5% wt/vol and autoclaved for sterilization. Next, 60μL of the silk solution and 20 μL of silica suspension were cast on the bottom of twenty-four-well TCP and left to dry for 24 hours in a fume hood. Plain silk film controls were obtained by casting 60 μL of silk solution only into TCP wells. Then, 2 mL of 70% methanol solution in water was added to each well to induce β-sheet formation in the silk films. The TCPs were left covered for 2 hours and then dried in air overnight. This step was used to generate silk films that were stable in an aqueous environment and suitable for cell culture. Films were sterilized with 70% ethanol, left to dry, and placed under UV light for 5 minutes in a laminar flow hood. TCP only was used as a control. Prior to cell seeding, 1 mL of cell culture medium was added to each well, soaked for 30 min, and then aspirated.

2.4. Human mesenchymal stem cells (hMSCs)

Bone marrow aspirate from a young healthy donor was obtained from Lonza (Walkersville, MD). Frozen low passage (2 or 3) hMSC stocks were thawed and suspended in growth medium containing high glucose Dulbecco's modified eagle medium (DMEM) supplemented with 10% fetal bovine serum, 1% antibiotic/antimycotic, 1% non-essential amino acids, and 10 ng basic fibroblast growth factor (bFGF). The cells were plated onto the silk and silk/silica films at a density of 5,000 cells/well in a 24-well plate and kept in a humidified incubator at 37°C and 5% CO_2. The cells were cultured in hMSC media until 85% confluency and then the medium was changed to an osteogenic medium containing high glucose Dulbecco's modified eagle medium (DMEM) supplemented with 10% fetal bovine serum, 1% antibiotic/antimycotic, 1% non-essential amino acids, 100 nM dexamethasone, 10 mM β-glycerolphosphate, and 0.05 mM L-ascorbic acid 2-phosphate. The medium was changed every 3–4 days. Cell growth and shape were monitored using a phase contrast light microscope (Carl Zeiss, Jena, Germany) equipped with a Sony Exwave HAD 3CCD (Sony Electronics Inc., USA) color video camera.

2.5. SEM

After 10 weeks of osteogenic culture, the basal parts of the tissue culture dishes were removed and fixed in 2.5% vol/vol glutaraldehyde solution in PBS for 30 minutes. Next, the samples were washed in DI water and dehydrated by 20 min incubation in a series of ethanol solutions in water (10%, 30%, 60%, 80%, 90%, 100% vol/vol). Samples were dried in air and imaged using FESEM.

2.6. Cell viability

The metabolic activity of cells after 10 weeks in osteogenic culture was quantified using the alamarBlue® assay according to the manufacturer's instructions. Briefly, 1 mL of a solution containing basic medium (DMEM supplemented with 1% antibiotic/antimycotic and 10% fetal bovine serum) with 10% alamarBlue® solution was added to 3 wells from each type of silk film, silk/silica film or TCP, and incubated for 2 h. A 100 μL aliquot was then taken from each well, and analyzed for fluorescence with excitation at 560 nm and recording the emission at 590 nm. Background fluorescence from the alamarBlue® solution alone was subtracted, and the sample values from 3 wells of each culture were averaged.

2.7. Gene expression using real–time RT-PCR analysis

After osteogenic culture, the cells from three separate wells of each type were lysed in 0.35 mL Buffer RLT (Qiagen, CA, USA) containing 10% mercaptoethanol, followed by shredding in a QIAshedder (Qiagen, CA, USA). RNA was isolated from the cells using an RNeasy Mini Kit (Qiagen, CA, USA). From this RNA, cDNA was synthesized using a High Capacity cDNA Reverse Transcription Kit (Applied Biosystems #4368814, MA, USA) following the manufacturer's instructions. The cDNA samples were analyzed for expression of collagen type I and bone sialoprotein relative to the GAPDH housekeeping gene using Assay-on-Demand™ Gene Expression kits with TaqMan® Universal PCR Master Mix (ABI, Applied Biosystems AoD probes, MA, USA). The data were analyzed using the ABI Prism 7000 Sequence Detection Systems software.

2.8. Collagen deposition

Collagen formation on the surface of experimental samples was analyzed by second harmonic generation (SHG) microscopy at weekly intervals for 10 weeks. The SHG micrographs were acquired using a Leica DMIRE2 microscope with a TCS SP2 scanner (Wetzlar, Germany). The system was equipped with a 10x (NA 0.3) dry, 20x (NA 0.7) dry and a 63x (NA 1.2) water immersion objective. The excitation light source was a Mai Tai tunable (710-920 nm) titanium sapphire laser emitting 100 fs pulses at 80 MHz (Spectra Physics, Mountain View CA). Samples were placed on culture dishes with number 1.5 cover glass bottoms (MATTEK, Ashland MA) and excited at 800 nm. SHG images were acquired in the forward direction through a bandpass filter centered at 400 nm (Chromahq400/20m-2p). Analysis was performed using the Leica Confocal Software (Wetzlar, Germany) and Matlab (Mathworks, Natick MA).

2.9. Collagen quantification

The total collagen content on the surface from three separate wells of each type was quantified using an hydroxyproline assay at 10 weeks of osteogenic culture using standard protocols [33]. Briefly, samples were collected and hydrolyzed overnight in 1 mL of 6 M HCl at 115°C before the acid was evaporated overnight at 100°C and the samples were rinsed with 1 mL of DI water twice with the water being removed by evaporation at 95°C. Next, the samples were prepared for colorimetric analysis with the addition of 0.05N chloramine-T, 3.15N perchloric acid, and Ehrlich's reagent. The hydroxyproline content was quantified using the absorbance measurement at 550 nm. The absorbance values were plotted against the hydroxyproline standards and the actual content of hydroxyproline in the experimental samples was extracted from the calibration curve.

2.10. Collagenase treatment of silk/silica films

The experimental wells were washed with PBS to remove the cell media and incubated for 2 days in Collagenase IA enzyme solution (1.0 U/mL) dissolved in 0.05 M sodium phosphate buffer (pH 7.0). Next, the samples were rinsed with PBS buffer and prepared for SEM analysis.

2.11. Analysis of silica concentration

Silica concentration within silk/silica films was determined before and after 10 weeks of osteogenic culture. Briefly, three wells with silk/silica films were incubated in 1 ml of 2 M sodium hydroxide solution overnight in order to resolubilize silica particles. Next, 1.0 ml of sample was diluted to 10.0 ml with distilled and de-ionized water. The solutions were analyzed by Inductively Coupled Plasma (ICP) spectrometer with argon plasma (Perkin Elmer, model Optima 2100 ICP, MA, USA) without further treatment using the emission band at 251.611 nm and comparing with a linearity plot constructed from 10 – 50 mg/l silica standards.

2.12. Statistical analysis

Results were analyzed using a two-sided Student's t-test in Excel with $p<0.05$ significance.

3. Results

3.1. Cell morphology, proliferation, and differentiation on silk/silica films

3.1.1. Cell morphology—The ability of silk/silica films to support the hMSC growth and osteogenic differentiation was assessed. The experimental setup is shown in Scheme 1. Control samples were TCP and also silk films only without addition of silica particles. Figure 1A shows the surfaces of the biomaterials with silica particles (24 nm, 500 nm, 2 μm) embedded into silk fibroin films. Cells adhered to the silk/silica films and expansion to 85% confluence was reached on day 5, the starting point of osteogenic differentiation. Cell morphology was examined by light microscopy at two time points, 5 days after cell seeding and 2 weeks after differentiation into osteogenic lineage. Before differentiation similar cell densities and morphologies were observed on all silk films, showing spindle-like shapes characteristic of undifferentiated fibroblastic hMSCs (Figure 1B). The growth rates were comparable with cells grown on TCP which on day 5 after seeding showed 95% confluence.

The effect of osteogenic differentiation on cell morphology (Figure 1C) was studied after 2 weeks of osteogenic stimulation. The cells spread evenly on silk film surfaces and formed a thin uniform layer. No differences in cell morphology were observed between the silk/silica samples and the control samples. The spindle-like cell morphology before differentiation changed to closely packed flattened cells organized on the surface in sheet-like fashion. After 10 weeks of osteogenic culture some detachment was observed for cells grown on TCP but not on silk/silica or silk only films.

3.1.2. Cell viability—In order to evaluate cell viability on silk/silica films the alamarBlue® assay was performed on cells at 10 weeks of culture. Results were compared with cells grown on silk film only and classical culture conditions on plastic with osteogenic stimuli as well as hMSCs grown on silk/24 nm silica in basic medium without osteogenic differentiation (Figure 2). Cells grown on silk/silica films for 10 weeks showed good viability with no statistical difference between cells grown on silk film only and TCP. The addition of silica particles to the silk films did not change the metabolic activity of cells. Additionally, hMSCs grown on silk/silica (24 nm) films in basic medium without osteogenic differentiation were used as a reference to establish if the addition of silica into the silk film would affect cell viability under standard culture conditions. The results showed comparable results for cell viability for all samples tested.

3.1.3. Osteogenic differentiation—To evaluate if addition of silica particles to the silk film could modulate hMSC differentiation, expression of bone-specific markers was quantified using real-time RT-PCR after 10 weeks of osteogenic culture. Figure 3A shows that bone sialoprotein (BSP) gene expression was upregulated when the cells were cultured on silk films with addition of 24 nm and 500 nm silica particles, with respect to the control samples. Higher

expression of BSP was also observed for silk/2 μm silica particles when compared to silk only and silk/silica 24 nm with undifferentiated hMSCs. Expression of collagen I was elevated on all silk/silica samples in osteogenic culture when compared to the controls.

3.2. The effects of silica in silk films on collagen deposition

Collagen deposition is a key event in bone remodeling since it constitutes the major organic component of the bone matrix. Fibrillar collagen has a highly non-centrosymmetric structure that is capable of emitting a strong and bright second harmonic generation signal (SHG) [34]. SGH to examine silk/silica samples, at one week intervals, for collagen deposition by cells during osteogenic stimulation. Figure 4 shows representative SHG images of collagen deposition on silk/silica films after 1 week, 2, 3, and 4 weeks respectively. Collagen deposition was found to increase steadily with each week in culture and after week 4 the SGH collagen signal was saturated. Additional evaluation was performed using a hydroxyproline assay at week 10 to quantify the total collagen content with respect to the cell number in each sample. The collagen content was higher for all samples containing silica with respect to the control experiments (Figure 4 Inset). These results show that silica presence in the samples induced higher deposition of collagen on the biomaterial surfaces.

3.3. The effects of silica in silk films on formation of extracellular matrix

Formation of mineralized matrix is a direct indication of osteogenic differentiation. Samples were evaluated for cell guided mineralization by SEM/EDAX analysis after 10 weeks in osteogenic culture. Figure 5 shows representative SEM images of a silk/silica 2 μm sample. Frame A of Figure 5 shows densely packed cells on the biomaterial surface with no additional mineral deposits on the cells surface. Nevertheless, mineral nodules with diameters of 527±50 nm were observed at the cell-film interface as shown in Figure 5B. The enlarged area in Figure 5C further reveals surface roughness of the particles and the presence of fibrous structures connecting the particles. Calcium incorporation was examined by EDAX mapping (Figure 6). Strong signals for Ca, P, and O were detected in EDAX maps that correspond to the areas covered with particles. This indicates the presence of a calcium and phosphorous containing material in the mineral nodules suggesting early bone apatite formation. Additionally, a strong carbon signal was detected arising from the silk film and a moderate signal for silicon resulting from residual silica particles (also a signal from oxygen, present in all constituent materials). All silk/silica samples showed similar trends, much lower mineralization was observed on silk films that did not contain silica and on TCP (results presented in supplementary data). Additionally, silk/silica samples were treated with collagenase to determine if the enzyme could digest the fibrillar structures connecting the mineral nodules. Figure 7 shows SEM images of a representative silk/silica 2 μm sample before (frame A,C) and after 2 days (frame B,D) of collagenase treatment. The fibrous structures disappeared rendering the surface with mineral nodules only suggesting that fibrils originated from collagen deposits. The size and shape of the mineral nodules did not change.

3.4. Silica particle degradation

The amount of silica within silk/silica films in the starting material and after *in vitro* studies was evaluated using ICP spectroscopy (Figure 8). The initial concentration of silica for 24 nm, and 2 μm silica particles embedded in silk film was ~50 mg/l, and for the 500 nm silica particles this was ~35 mg/l. The silica concentrations decreased significantly after 10 weeks of osteogenic culture to ~10 mg/l of residual silica (24 nm, 2 μm) and ~6 mg/l (500 nm) within silk/silica sample. These findings indicate that silica particles are degrading slowly over time under physiological conditions.

4. Discussion

Silica based composites have been extensively studied as bone implant materials due to their osteoinductive properties and biocompatibility. However, the lack of biodegradability or very slow degradation of silica-based fillers establishes a barrier for tissue regeneration *in vivo* [35,36]. In order to overcome this problem chemically synthesized nanoscale silica particles were incorporated into biodegradable silk matrix materials. The advantage of silica particles is their small size that offers improved degradation through amorphous silica dissolution, which is difficult to achieve for a high mass of dense, low surface area bioactive glass. We examined three different sizes of silica particles: 24 nm, 500 nm, and 2 μm embedded in silk film matrices with respect to their ability to stimulate new bone formation using hMSCs in an *in vitro* model system, subjected to osteogenic differentiation.

All films were treated with methanol to induce β-sheet secondary structures within the silk to improve mechanical properties and foster insolubility in water, desirable properties for biomaterials used in biological systems [37]. It has been previously shown that cells adhere well to silk films [38]. The addition of silica did not change the attachment of hMSCs to the silk films and cells showed good proliferation rates comparable to TCP. Also, we observed cell viability when subjected to osteogenic stimuli for prolonged periods of time which suggests biocompatibility of the silk/silica biomaterials. Differences in morphology were seen as the hMSCs were subjected to osteogenic differentiation, with cell flattening, horizontal elongation, and close adherence to one another. After 10 weeks in osteogenic culture cells maintained good adherence to the silk/silica films, while some detachment and formation of cell clusters was observed on the TCP.

Dissolution products of bioactive glasses can influence gene expression of host cells [39,40]. Constitutive ions of bioactive glasses regulated the expression of genes responsible for the growth and differentiation of osteoblasts, production of extracellular matrix, and promotion of cell-cell and cell-matrix adhesion. Similarly, the present studies showed that the presence of a silica component in the silk films led to high expression levels of bone sialoprotein (BSP), an osteoblast differentiation marker, for all silk/silica samples in osteogenic culture. The BSP was upregulated on the silk films that contained 24 nm and 500 nm silica particles when compared to cells grown on silk film only, TCP, and also silk/silica 24 nm particles with undifferentiated hMSCs. The low expression of BSP on silk/silica 24 nm with undifferentiated hMSCs suggests that the presence of silica only within the silk film was not sufficient to induce BSP gene upregulation if the hMSCs were not subjected to additional osteogenic stimuli. BSP levels were higher for cells cultured on silk/silica 2 μm films when compared to silk only and silk/silica 24 nm hMSCs. Additionally, overexpression of collagen type I (Col 1), the second osteogenic marker, was observed for all silk/silica containing samples when compared to all control experiments. The upregulation of BSP and Col 1 on silk/silica biomaterials in osteogenic culture suggests the influence of silica presence on gene expression towards upregulation of osteogenesis.

The process of bone formation is initiated with matrix deposition in a randomly oriented pattern, synthesized by differentiating mesenchymal cells that have just differentiated to osteoblasts [41]. The early bone matrix is further replaced with lamellar structures during bone development. It was found that silica species promoted an early phase of collagen fibril self-assembly affecting the formation of collagen fibril “nuclei” through possible hydrogen bonding and hydrophilic interactions between collagen helices [42,43]. We investigated collagen formation in experimental samples with hMSCs subjected to osteogenic stimuli for a period of 10 weeks. The results showed that much higher collagen deposition was observed when silica particles were present within the material. These findings suggest that the silica component stimulates increased collagen deposition and highlights the functional properties

of these silk/silica biomaterials. The undifferentiated hMSCs did not show increased collagen production, as expected. The results for total collagen content were normalized with respect to the cell number in each experimental well to avoid error due to the differences in cell density in each sample.

The main hallmark of osteogenic differentiation is extracellular matrix formation, also a prerequisite for successful bone remodeling *in vivo* [44]. We assessed cell-substrate interactions and mineral phase deposition in our experimental substrates. After 10 weeks we observed nodular mineral deposits on all silk/silica biomaterials surface. These deposits tested positive for the presence of calcium and phosphorous which suggests early apatite formation. Samples not containing silica did not produce nodular structures, although some very limited deposits with calcium and phosphorous at the cell-surface interface. This finding additionally provides evidence for the influence of silica on osteogenesis and its ability to promote cellular mineral deposition on the biomaterial surface.

Additionally, we observed fibrillar structures associated with the mineral nodules. It has been previously shown that collagen can propagate mineral deposition resulting in mineralized structures intercalated and bound to collagen fibers [45]. Apatite crystals have been found to nucleate in a highly organized manner along the collagen fiber length [46,47], as well as on the collagen fibril surface [48]. In the present study, the samples which exhibited high mineral-fibrillar content were placed in collagenase solution for two days to investigate if this could lead to fiber dissolution. After treatment was complete we still observed the presence of mineral particles on the silk/silica surface but the fibrillar structures had disappeared. This finding suggests that the fibers associated with the mineral nodules originate from collagen.

One of the most important and highly sought features of biomaterials is their biodegradability that enables replacement of implant material with newly formed functional tissue. Studies using silk have shown that the materials slowly degrade in vitro and in vivo at rates suitable for applications in biological systems [49-52]. We also studied silica particle degradation within silk films during *in vitro* studies of hMSCs in osteogenic culture. We found ~5-fold decrease in silica content within silk/silica films over a 10 week period, indicating slow dissolution over time. This finding indicates the importance of particle sizes used, where the high surface area of amorphous silica particles leads to dramatic changes in material properties when compared to the non-degradable silica-based bulk of bioactive glass. Also, the nanometer size range of silica particles should facilitate entry into macrophages and other cells for further bone remodeling.

5. Conclusions

Silica particles incorporated into silk films provided a family of composite biomaterials for bone tissue engineering. The studies showed that good hMSC proliferation rates as well as high cell viability for all silk/silica composite samples. Moreover, the presence of silica in the samples led to the upregulation of osteogenic markers and increased the formation of a collagen/calcium phosphate extracellular matrix, indicating the osteoinductive properties of the biomaterial. Also, the silica particles were biodegradable.

Supplementary Material

Refer to Web version on PubMed Central for supplementary material.

Acknowledgments

This work was performed in part at the Center for Nanoscale Systems (CNS), a member of the National Nanotechnology Infrastructure Network (NNIN) at Harvard University, which is supported by the National Science

Foundation under NSF award no. ECS-0335765. The authors thank the NIH (DE017207, EB003210, EB002520) for support of the project.

References

1. Sakiyama-Elbert SE, Hubbell JA. Functional biomaterials: design of novel biomaterials. Annu Rev Mater Res 2001;31:183–201.
2. Kokubo T, Kim HM, Kawashita M. Novel bioactive materials with different mechanical properties. Biomaterials 2003;24:2161–2175. [PubMed: 12699652]
3. Ter Brugge PJ, Jansen JA. In vitro osteogenic differentiation of rat bone marrow cells subcultured with and without dexamethasone. Tissue Eng 2002;8:321–331. [PubMed: 12031120]
4. Stiehler ML, Lind M, Mygind T, Baatrup A, Dolatshahi-Pirouz A, Li H, et al. Morphology, proliferation, and osteogenic differentiation of mesenchymal stem cells cultured on titanium, tantalum, and chromium surfaces. J Biomed Mat Res Part A 2007;86:448–458.
5. Bluteau G, Pilet P, Bourges X, Bilban M, Spaethe R, Daculsi G, et al. The modulation of gene expression in osteoblasts by thrombin coated on biphasic calcium phosphate ceramic. Biomaterials 2006;27:2934–2943. [PubMed: 16436294]
6. Hee C, Jonikas M, Nicoll S. Influence of three-dimensional scaffold on the expression of osteogenic differentiation markers by human dermal fibroblasts. Biomaterials 2006;27:875–884. [PubMed: 16102817]
7. Lovett M, Cannizzaro C, Daheron L, Messmer B, Vunjak-Novakovic G, Kaplan DL. Silk fibroin microtubes for blood vessel engineering. Biomaterials 2007;28:5271–5279. [PubMed: 17727944]
8. Minoura N, Tsukada M, Nagura M. Physico-chemical properties of silk fibroin membrane as a biomaterial. Biomaterials 1990;11:430–434. [PubMed: 2207234]
9. Jin H-J, Park J, Karageorgiou V, Kim U-J, Valluzzi R, Cebe P, et al. Water-stable silk films with reduced beta-sheet content. Adv Funct Mater 2005;15:1241–1247.
10. Winkler S, Wilson D, Kaplan DL. Controlling beta-sheet assembly in genetically engineered silk by enzymatic phosphorylation/dephosphorylation. Biochemistry 2000;39:12739–12746. [PubMed: 11027155]
11. Matsumoto A, Chen J, Collette AL, Kim UJ, Altman GH, Cebe P, et al. Mechanisms of silk fibroin sol-gel transitions. J Phys Chem B 2006;110:21630–21638. [PubMed: 17064118]
12. Drummy LF, Farmer BL, Naik RR. Correlation of the B-sheet crystal size in silk fibers with the protein amino acid sequence. Soft Matter 2007;3:877–882.
13. Murphy AR, St John P, Kaplan DL. Modification of silk fibroin using diazonium coupling chemistry and the effects on hMSC proliferation and differentiation. Biomaterials 2008;29:2829–2838. [PubMed: 18417206]
14. Tamada Y. New process to form a silk fibroin porous 3-D structure. Biomacromolecules 2005;6:3100–3106. [PubMed: 16283733]
15. Wang Y, Blasioli DJ, Kim HJ, Kim HS, Kaplan DL. Cartilage tissue engineering with silk scaffolds and human articular chondrocytes. Biomaterials 2006;27:4434–4442. [PubMed: 16677707]
16. Jin HJ, Fridrikh SV, Rutledge GC, Kaplan DL. Electrospinning Bombyx mori silk with poly(ethylene oxide). Biomacromolecules 2002;3:1233–1239. [PubMed: 12425660]
17. Kim UJ, Park J, Li C, Jin HJ, Valluzzi R, Kaplan DL. Structure and properties of silk hydrogels. Biomacromolecules 2004;5:786–792. [PubMed: 15132662]
18. Preghenella M, Pezzotti G, Migliaresi C. Comparative Raman spectroscopic analysis of orientation in fibers and regenerated films of Bombyx mori silk fibroin. J Raman Spectrosc 2007;38:522–536.
19. Sofia S, McCarthy MB, Gronowicz G, Kaplan DL. Functionalized silk-based biomaterials for bone formation. J Biomed Mater Res 2001;54:139–148. [PubMed: 11077413]
20. Altman GH, Diaz F, Jakuba C, Calabro T, Horan RL, Chen J, et al. Silk-based biomaterials. Biomaterials 2003;24:401–416. [PubMed: 12423595]
21. Wang Y, Kim HJ, Vunjak-Novakovic G, Kaplan DL. Stem cell-based tissue engineering with silk biomaterials. Biomaterials 2006;27:6064–6082. [PubMed: 16890988]
22. Panilaitis B, Altman GH, Chen J, Jin HJ, Karageorgiou V, Kaplan DL. Macrophage responses to silk. Biomaterials 2003;24:3079–3085. [PubMed: 12895580]

23. Karlsson KH, Froberg K, Ringbom T. A structural approach to bone adhering of bioactive glasses. Journal of Non-Crystalline Solids 1989;112:69–72.
24. Lopez-Noriega A, Arcos D, Izquierdo-Barba I, Sakamoto Y, Terasaki O, Vallet RM. Ordered mesoporous bioactive glasses for bone tissue regeneration. Chem Mater 2006;18:3137–3144.
25. Bosetti M, Cannas M. The effect of bioactive glasses on bone marrow stromal cells differentiation. Biomaterials 2005;26:3873–3879. [PubMed: 15626435]
26. Tan W, Wang K, He X, Zhao X, Drake T, Wang L, et al. Bionanotechnology based on silica nanoparticles. Med Res Rev 2004;24:621–638. [PubMed: 15224383]
27. Rosenholm J, Sahlgren C, Linden M. Cancer-cell targeting and cell-specific delivery by mesoporous silica nanoparticles. J Mater Chem 2010;20:2707–2713.
28. Galagudza M, Korolev D, Sonin D, Postnov V, Papayan G, Uskov I, et al. Targeted drug delivery into reversibly injured myocardium with silica nanoparticles: surface functionalization, natural biodistribution, and acute toxicity. Int J Nanomedicine 2010;5:231–237. [PubMed: 20463939]
29. Au AY, Au RY, Al-Talib TK, Eves B, Frondoza CG. Consil bioactive glass particles enhance osteoblast proliferation and maintain extracellular matrix production in vitro. J Biomed Mater Res 2008;86:678–684.
30. Kim HW, Song JH, Kim HE. Bioactive glass nanofiber-collagen nanocomposite as a novel bone regeneration matrix. J Biomed Mat Res 2006;79:698–705.
31. Couto DS, Hong Z, Mano JF. Development of bioactive and biodegradable chitosan-based injectable systems containing bioactive glass nanoparticles. Acta Biomater 2009;5:115–123. [PubMed: 18835230]
32. Stober W, Fink A, Bohn E. Controlled growth of monodisperse silica spheres in the micron size range. J Colloid Interface Sci 1968;26:62–69.
33. Reddy GK, Enwemeka CS. A simplified method for the analysis of hydroxyproline in biological tissues. Clin Biochem 1996;29:225–229. [PubMed: 8740508]
34. Bayan C, Levitt JM, Miller E, Kaplan DL, Georgakoudi I. Fully automated, quantitative, noninvasive assessment of collagen fiber content and organization in thick collagen gels. J Appl Phys 2009;105:102042–102042-11.
35. Ohtsuki C, Kamitakahara M, Miyazaki T. Bioactive ceramic-based materials with designed reactivity for bone tissue regeneration. J R Soc Interface 2009;6:S349–S360. [PubMed: 19158015]
36. Hill R. An alternative view of the degradation of bioglass. J Mater Sci Lett 1996;15:1122–1125.
37. Taketani I, Nakayama S, Nagare S, Senna M. The secondary structure control of silk fibroin thin films by post treatment. Appl Surf Sci 2005;244:623–626.
38. Vepari C, Kaplan DL. Silk as a Biomaterial. Prog Polym Sci 2007;32:991–1007. [PubMed: 19543442]
39. Christodoulou I, Buttery LD, Tai G, Hench LL, Polak JM. Characterization of human fetal osteoblasts by microarray analysis following stimulation with 58S bioactive gel-glass ionic dissolution products. J Biomed Mater Res Part B: Appl Biomater 2006;77B:431–446. [PubMed: 16333845]
40. Bombonato-Prado KF, Bellesini LS, Junta CM, Marques MM, Passos GA, Rosa AL. Microarray-based gene expression analysis of human osteoblasts in response to different biomaterials. J Biomed Mat Res Part A 2008;88:401–408.
41. Shapiro F. Bone development and its relation to fracture repair. The role of mesenchymal osteoblasts and surface osteoblasts. Eur Cell Mater 2008;15:53–76. [PubMed: 18382990]
42. Eglin D, Coradin T, Giraud Guille MM, Helary C, Livage J. Collagen-silica hybrid materials: sodium silicate and sodium chloride effects on type I collagen fibrillogenesis. Biomed Mater Eng 2005;15:43–50. [PubMed: 15623929]
43. Eglin D, Shafran KL, Livage J, Coradin T, Perry CC. Comparative study of the influence of several silica precursors on collagen self-assembly and of collagen on ‘Si’ speciation and condensation. J Mater Chem 2006;16:4220–4230.
44. Deschaseaux F, Sensebe L, Heymann D. Mechanisms of bone repair and regeneration. Trends Mol Med 2009;15:417–429. [PubMed: 19740701]
45. Barragan-Adjemian C, Nicolella D, Dusevich V, Dallas MR, Eick JD, Bonewald LF. Mechanism by which MLO-A5 late osteoblasts/early osteocytes mineralize in culture: similarities with mineralization of lamellar bone. Calcif Tissue Int 2006;79:340–353. [PubMed: 17115241]

46. Landis WJ. An overview of vertebrate mineralization with emphasis on collagen-mineral interaction. Gravit Space Biol Bull 1999;12:15–26. [PubMed: 11541779]

47. Glimcher MJ. Mechanism of calcification: role of collagen fibrils and collagen-phosphoprotein complexes in vitro and in vivo. Anat Rec 1989;224:139–153. [PubMed: 2672881]

48. Landis WJ, Hodgens KJ, Song MJ, Arena J, Kiyonaga S, Marko M, et al. Mineralization of collagen may occur on fibril surfaces: evidence from conventional and high-voltage electron microscopy and three-dimensional imaging. J Struct Biol 1996;117:24–35. [PubMed: 8776885]

49. Li M, Ogiso M, Minoura N. Enzymatic degradation behavior of porous silk fibroin sheets. Biomaterials 2003;24:357–365. [PubMed: 12419638]

50. Wang Y, Rudym DD, Walsh A, Abrahamsen L, Kim HJ, Kim HS, et al. In vivo degradation of three-dimensional silk fibroin scaffolds. Biomaterials 2008;29:3415–3428. [PubMed: 18502501]

51. Arai T, Freddi G, Innocenti R, Tsukada M. Biodegradation of Bombyx mori silk fibroin fibers and films. J Appl Pol Sci 2004;91:2383–2390.

52. Horan RL, Antle K, Collette AL, Wang Y, Huang J, Moreau JE, et al. In vitro degradation of silk fibroin. Biomaterials 2005;26:3385–3393. [PubMed: 15621227]

Scheme 1.

Experimental setup for silk/silica films *in vitro* studies using hMSCs culture with osteogenic differentiation.

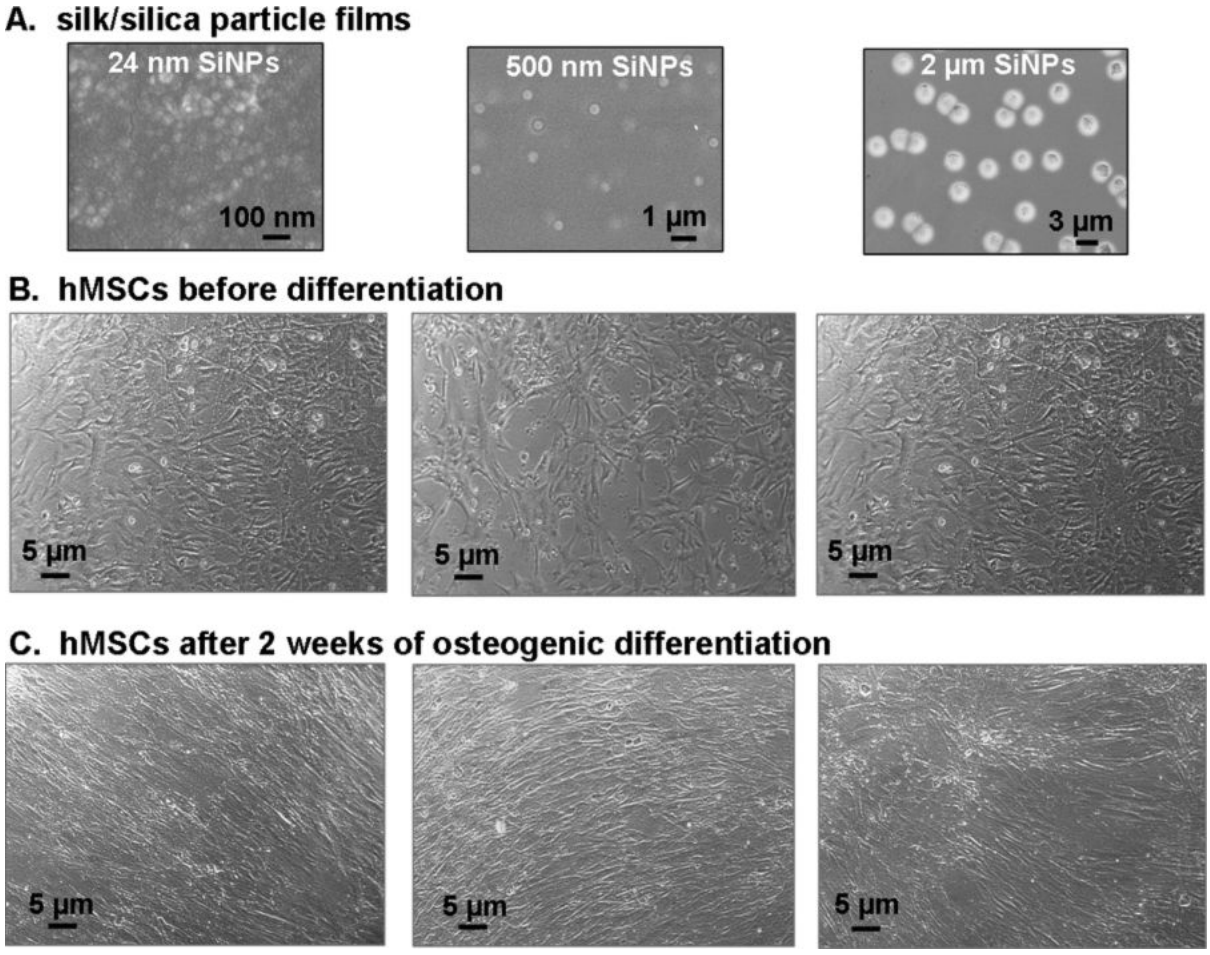

Figure 1.
(A) SEM images of silk films with three different sizes of silica particles used in hMSCs in vitro study. (B) Optical microscopy images of hMSCs grown on silk/silica films at day 5 after seeding in basic growth medium. The sample lineup corresponds to the silk/silica films in part A. (C) Optical microscopy images of hMSCs on silk/silica films after 2 weeks of osteogenic culture.

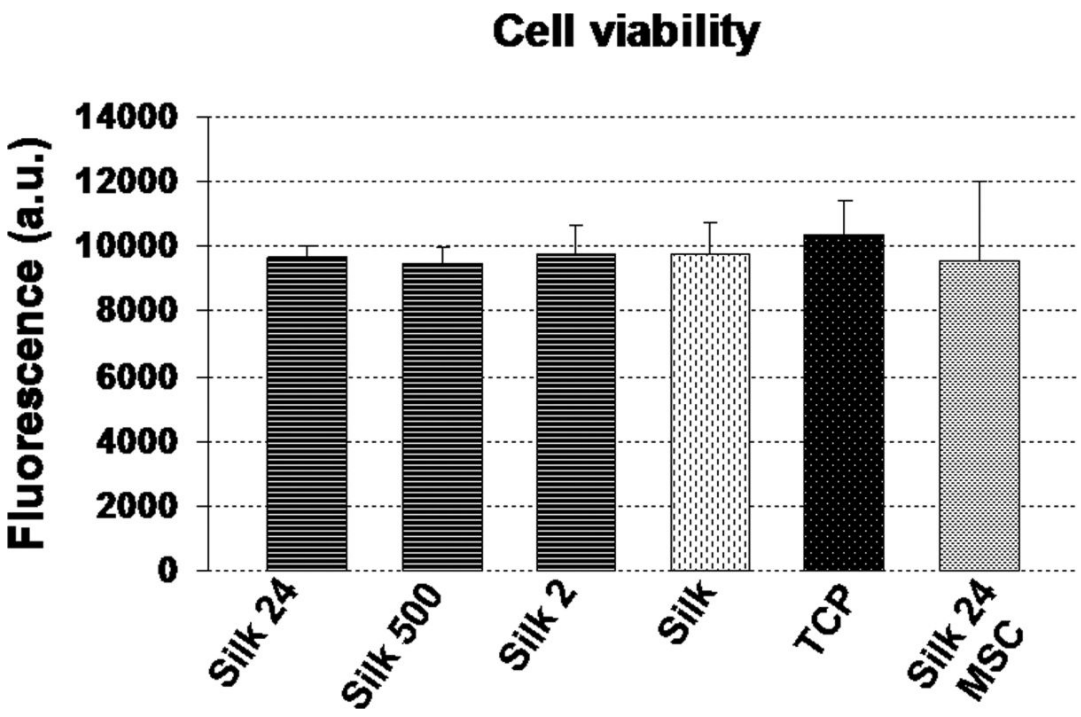

Figure 2.

AlamarBlue metabolic activity assay for cells in growth medium after 10 weeks of osteogenic culture. Each column represents the mean and standard deviation of *N=3* independent cultures, and corrected for the background fluorescence of the dye alone.

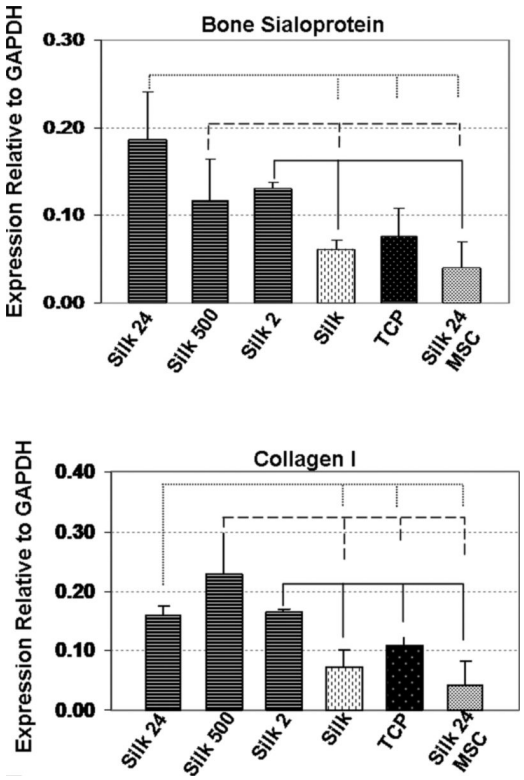

Figure 3.

Osteogenic gene expression of cells grown on silk/silica films (Silk 24, Silk 500, and Silk 2) or silk only (Silk) and tissue culture plastic (TCP) after exposure to osteogenic stimulants for 10 weeks as compared to cells in control medium (Silk 24 MSC). Each column represents the mean and standard deviation of N = 3 independent cultures. $P<0.05$.

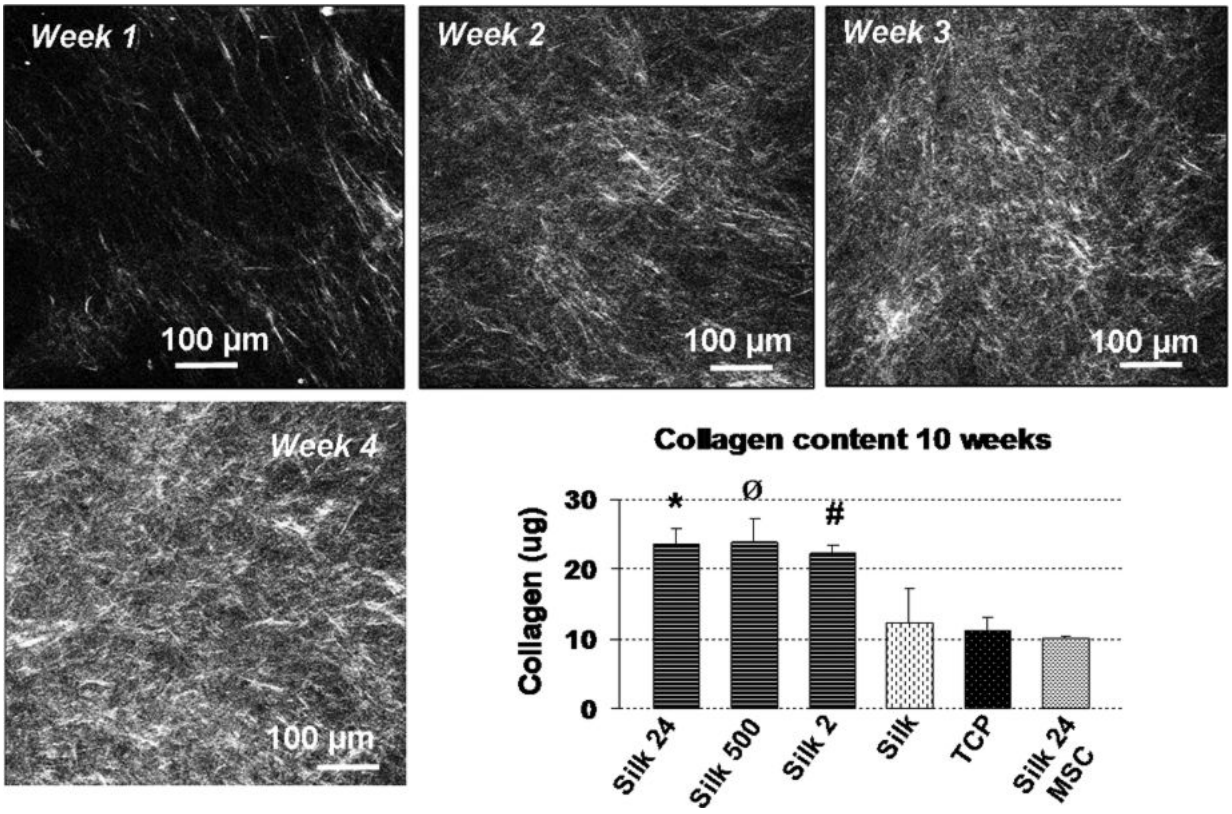

Figure 4.

Successive collagen deposition on silk/silica 24 nm film imaged with second harmonic generation at week 1, 2, 3, and 4. Graph inset represents the mean and standard deviation of total collagen deposition at week 10 of *N=3* independent cultures, and normalized with respect to the cell number in each culture. P<0.05.

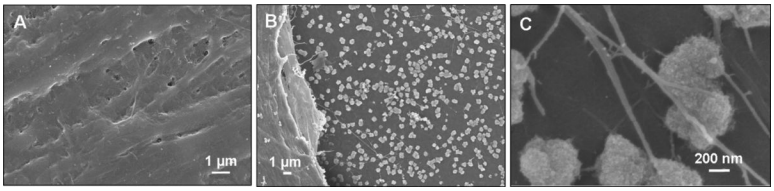

Figure 5.
SEM images of fixed silk/silica 2 μm samples after 10 weeks of hMSCs osteogenic culture. (A) surface of the cells, (B) cell-surface interface, and (C) zoomed in area showed mineral deposits on the silk/silica film surface.

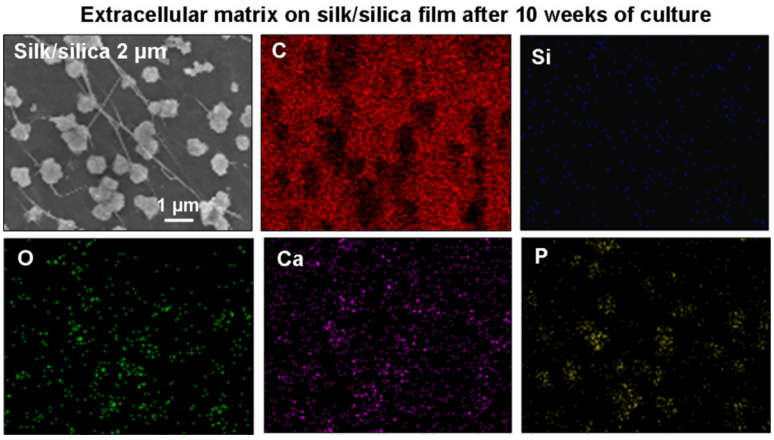

Figure 6.
SEM image and EDAX mapping of silk/silica 2 μm film surface after 10 weeks of hMSCs osteogenic culture.

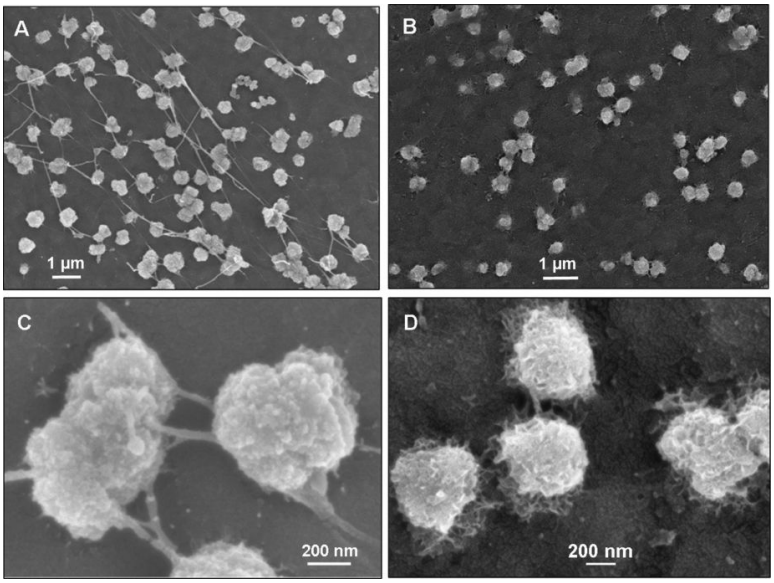

Figure 7.
SEM images of silk/silica 2 μm film surface before (frames A, C) and after (frames B, D) 2 days of collagenase treatment.

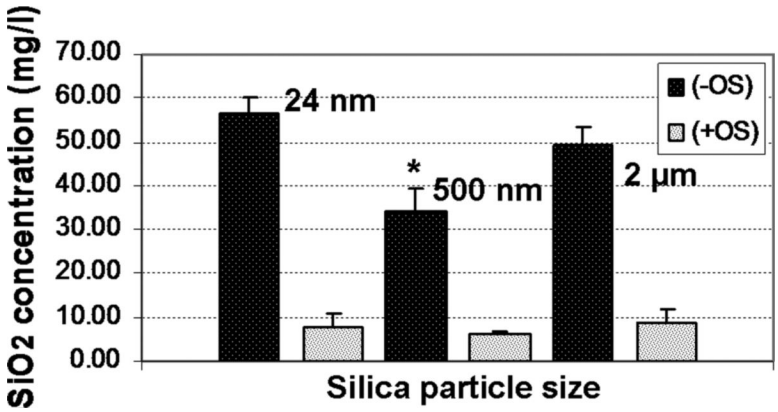

Figure 8.
Silica particle degradation in silk/silica films before (–OS) and after (+OS) 10 weeks of osteogenic hMSCs culture.